Research Article

Synthesis and swelling behavior of super-absorbent soluble starch-*g*-poly(AM-*co*-NaAMC$_{14}$S) through graft copolymerization and hydrolysis[†]

Guihong Lan[a,*], Ming Zhang[a], Yongqiang Liu[b], Haiyan Qiu[a], Songsong Xue[a], Tailiang Zhang[a,c], Qianxia Xu[a]

a College of Chemistry and Chemical Engineering, Southwest Petroleum University, Chengdu 610500, PR China

b Faculty of Engineering and the Environment, University of Southampton, Southampton SO17 1BJ, United Kingdom.

c Sichuan Kuineng Environmental Protection Technology Co. LTD, Chengdu 610500, PR China.

* Correspondence author at: No. 8 Xindu District, Chengdu 610500, PR China.

Fax: +86 283037306. E-mail address: guihonglan416@sina.com (G. Lan)

[†]This article has been accepted for publication and undergone full peer review but has not been through the copyediting, typesetting, pagination and proofreading process, which may lead to differences between this version and the Version of Record. Please cite this article as doi: [10.1002/star.201800272].

Received: September 29, 2018 / Revised: December 17, 2019 / Accepted: December 24, 2018

Abstract

By introducing sodium 2-acrylamido-tetradecanesulfonate (NaAMC$_{14}$S) to graft copolymerization of soluble starch and acrylamide (AM), a novel super absorbent resin (SAR) of soluble starch-*g*-poly(AM-*co*-NaAMC$_{14}$S) (SR-14) was synthesized. Polymer gels were hydrolyzed with sodium hydroxide (NaOH) to convert the function group -CONH$_2$ to -COO$^-$. The structures and qualitative changes of the polymer gels were characterized through Fourier transform infrared spectroscopy (FT-IR), scanning electron microscopy (SEM), Elemental analysis and Rheometer. Results showed the polymer gels through the hydrolysis by NaOH increased the water absorbency of the final SR-14 resin from 31.71 g/g to 1183.43 g/g as the degree of hydrolysis (DH) increased from 0 % to 80 %. Drastic increases in the storage and loss modulus of SR-14 reflected the intensive molecular structural changes induced by the addition of NaAMC$_{14}$S. The changes in the molecular structures of SR-14 could be attributed to hydrophobic associations among long-chain alkane.

Soluble starch-*g*-poly(AM-*co*-NaAMC$_{14}$S) exhibited the maximum water absorbency of 2536.77 g/g in distilled water and 92.98 g/g in 0.9 wt.% NaCl solution. In the absence of NaAMC$_{14}$S, however, the water absorbency of soluble starch-*g*-poly(AM) decreased to 1222.27 g/g in distilled water and to 62.29 g/g in 0.9 wt.% NaCl solution. Results indicated that NaAMC$_{14}$S has potential applications as a material that could enhance the water absorbency of SAR.

Keywords: Soluble starch, acrylamide, hydrophobic monomers, super absorbent resin.

1. Introduction

Super absorbent resins (SAR), are novel functional polymers with high crosslinking densities and numerous hydrophilic groups, such as -COOH, and -OH. The water absorbency mechanism and capacities of these resins are distinct from those of traditional absorbent materials, for example, cotton and sponge [1,2]. Super absorbent resins have water absorption capacities of hundreds to thousands of times of their own weights given their abundant hydrophilic groups and net structures. The high water retention rates of SAR in saline environments can be ascribed to the chemical bonds of their functional groups [3]. Native carbohydrates, such as β-cyclodextrin, carboxymethylcellulose, and starch, are commonly applied to synthesize SAR to enhance the absorption capacity and biodegradability. Nakason subjected cassava starch and acrylamide (AM) to photopolymerization to prepare SAR with the maximum absorption of 1452 g/g and 83 g/g for distilled water and saline solution, respectively [4]. Huo increased the water absorption of starch and sodium acrylate system in distilled water and 0.9 wt.% NaCl solution to 2017.8 g/g and 89.7 g/g, respectively, by introducing poly vinylpyrrolidone (PVP) [5]. Li performed an orthogonal experiments to optimize the synthesis conditions for konjac glucomannan-acrylic acid-acrylamide polymers, the polymers had maximum absorption of 1941 g/g in distilled water and 93 g/g in physiological saline [6]. There still remains massive potentials for the development of superior products through currently available simple synthesis methods.

Soluble starch is a cationic starch that is derived from the etherification of the branched hydroxyl -OH chains of rice starch. It consists of two six-membered rings connected by an ether bond. Other sites in the rings are occupied by -OH groups. Soluble starch has been to synthesize different SAR because of its cheapness and chemical structure. The salt and heat resistances of polymers can be improved through the introduction of hydrophobic monomers comprising long hydrocarbon chains and nonpolar groups. These hydrophobic monomers contain polymerizable C=C, and its structures are composed of hydrophobic tails and hydrophilic groups [7,8]. Micellar nanostructures with different morphologies could form through hydrophobic intramolecular associations and intermolecular interactions with the addition of hydrophobic monomers to the polymerization system [9,10]. Hydrophobic monomers are widely used to synthesize polymer flooding agents and to improve the temperature and salt resistance of different agents. Gao obtained P(AM-NaAMC$_{14}$S), a hydrophobically associating polymer with stronger positive salinity sensitivity than conventional polyacrylamide (PAM). Wang introduced the hydrophobic monomer 2-acrylamido-2-methyl propane sulfonic acid (AMPS) to enhance the intrinsic viscosity of silicone modified hydrophobically associating polyacrylamide [11]. These results indicate that hydrophobic monomers may be introduced to synthesize SAR with excellent absorbency capacity.

Acrylic acid (AA) and acrylamide (AM) are two types of monomers that are extensively utilized to synthesize SAR because of their simple structures and functional group C=C. Sodium hydroxide (NaOH) is added during polymer synthesis with AA and AM to adjust the neutralization degree of the solution to enable the grafting of other monomers [12,13]. The use of AM alone in the synthesis of SAR, however, has not been properly investigated.

This study aims to investigate the water absorbency improvement of hydrolysis and hydrophobic monomer introduction, the two critical steps in the synthesis of a novel SAR from soluble starch and AM system. Hydrolysis was necessary for converting $-CONH_2$ to $-COO^-$ of the AM system. The enhancements in the water absorbency capacities of SAR synthesized under different hydrolysis conditions were experimentally verified. Sodium 2-acrylamido-tetradecanesulfonate ($NaAMC_{14}S$) was introduced as a hydrophobic monomer to the soluble starch and AM system. The effect of $NaAMC_{14}S$ on enhancing the water absorbency of SAR was investigated. Meanwhile, the mechanism underlying the adsorption behaviors of SAR immersed in distilled water and in 0.9 wt.% NaCl solution were evaluated.

2. Materials and Methods

2.1. Materials

Soluble starch (CAS number: 9005-84-9) procured from Kelong Chemical Reagent Plant (Chengdu, China) was used without purification. Acrylamide (AM, CAS number: 201-173-7), Ammonium persulfate (APS, CAS number: 231-786-5), *N*,*N*-methylene bisacrlamide (MBA, CAS number: 110-26-9). Sodium 2-acrylamido-tetradecanesulfonate ($NaAMC_{14}S$, average molecular weight: 351 Da) was purchased from Sichuan Guangya Polymer Chemical Corporation Ltd. (Sichuan, China). Other chemicals used were all analytical grade, all solutions used were prepared with Wahaha pure water purchased from Wahaha Qili food Corporation Ltd. (Sichuan, China).

2.2. Preparation of soluble starch-*g*-poly(AM-*co*-$NaAMC_{14}S$)

Super absorbent resin was synthesized in solution through graft polymerization by using soluble starch as the grafted carbon skeleton, AM as the grafted bridge, $NaAMC_{14}S$ as the performance enhancing monomer, APS as the redox initiator, and MBA as the crosslinking agent. First, 10 g of solid monomers were dissolved in 40 mL of Wahaha pure water. Soluble starch and 20 mL of pure water were stirred magnetically at 70 ℃. Other monomers, including AM, $NaAMC_{14}S$, and MBA were dissolved in 10 mL pure water. The APS solution was prepared with the concentration of 5000 mg/L. After 15 min of stirring, the APS solution and other monomers solution were added to the starch solution. The pH of the solution was immediately adjusted to neutral with 1 mol/L NaOH. The mixed solution gelled after more than 10 minutes. Upon gelation, the magnetic stirrer was switched off, the gel was maintained at 70 ℃ for 3 h. The gel was cooled down to the ambient temperature and then cut into small cubes by using scissors. Later, m_1 g of grainy gel and m_2 g of NaOH were thoroughly mixed and placed in a resealable bag. Here, m_1 and m_2 follow the equation 1. The bag was placed in an electrothermal blowing dry box at 90 ℃ for 3 h. The obtained hydrogel products were dried at 90 ℃ for 24 h. Finally the dried soluble starch-*g*-poly(AM-*co*-$NaAMC_{14}S$) was obtained and designated as SR-14.

$$\mathrm{m}_2 = m_1 \times 20\% \times \mathrm{f} \times 40 \div 71 \qquad (1)$$

where m_1 and m_2 are the weight of the grainy gel and NaOH, g; 20 % is the proportion of intermediate products in the gel; f is the degree of hydrolysis (DH) of the intermediate products; 40 and 71 are the relative molecular masses of NaOH and AM, respectively, g/mol.

2.3. Measurement of water absorbency

Absorption rates were evaluated by analyzing the water absorbency of powered SAR prepared under different reaction conditions. Approximately 0.1 g of the powdered resin was immersed in 250 mL distilled water for 5 h at room temperature. The residual water was removed by filtration with a 40-mesh nylon fine screen. Water absorbency was calculated in accordance with the following equation 2：

$$Q_a = \frac{W_2 - W_1}{W_1} \qquad (2)$$

where Q_a is water absorbency defined as grams of deionized water per grams of sample, g/g; W_1 and W_2 are the weight of samples before and after swelling in aqueous solutions, respectively, g.

2.4. characterization of SAR

Infrared spectra (IR) was recorded on a Fourier-transform infrared spectroscopy (FT-IR) (WQF 520, Beijing). Samples for IR were prepared with KBr. Polymeric gel and swollen SAR specimens for scanning electron microscopy (SEM, Quanta 450, America) observations were dried in liquid nitrogen after immersion in distilled water by using a vacuum freeze dryer. The dried specimens were placed carefully on conducting glue coated with Au vapor to confer conductivity and analyzed on a Quanta 450 SEM operated at 20 kV. The samples were subjected to elemental composition analysis before and after hydrolysis by using an elemental analyzer (Var10EL-III, Germany). The rheological properties of the polymers were investigated with HAAKE MARS III Rheometer (HAAKE, Germany). An ALLIED camera was used to photograph the expansion behavior of SR-14. Images were merged by using Photoshop software.

3. Results and discussion

3.1. Characterization of SAR

3.1.1. FT-IR analysis

The grafted soluble starch, hydrophobic NaAMC$_{14}$S monomer, and final SR-14 product were subjected by FT-IR analysis. As shown in Fig. 1, the characteristic bands of soluble starch appear at 1155, 1094 and 971 cm^{-1} in the spectrum of SR-14 after copolymerization and are attributed to the stretching vibrations of C-O-C (Fig. 1a and c). The presence of these bonds indicates that the soluble starch has become the carbon skeleton of SR-14 [14]. The appearance of the main characteristic peaks of NaAMC$_{14}$S at 2915 cm^{-1} (-CH$_2$ asymmetric stretching), 2850 cm^{-1} (C-H stretching), 1211 and 1047 cm^{-1} (R-SO$_3^-$M$^+$ stretching, where M$^+$ represents metal ions) in the spectrum of SR-14 (Fig. 1b) indicates that NaAMC$_{14}$S has grafted onto the SR-14 backbone [15]. In addition, peaks corresponding to the intramolecular coupling of the hydrogen bonds of -OH and the O-H stretching vibration appear at 3500 cm^{-1} and 3440 cm^{-1}, respectively. The peak at 3607 cm^{-1} is assigned to the primary alcohol hydroxyl on the soluble starch skeleton. Three new bands at 1685, 1550 and 1456 cm^{-1} ascribe to the -COOH and -COO$^-$, appeared in the spectrum of SR-14. These results are attributed to the hydrolysis process of the intermediate gel products by NaOH, where $-CONH_2$ is converted to $-COO^-$ or -COOH [16].

Figure 2 provides a schematic of the synthesis of SR-14. Acrylamide is the key monomer that grafted on soluble starch. Soluble starch is added to transport the C=C groups of AM into C-C under the support of the initiator APS. Free radicals formed on the initiated chain, and numerous of free monomers participate in chain growth [17,18]. Simultaneously, under the action of the crosslinking agent MBA, ~~a~~ three dimensional network is formed by numerous long chains. Hydrophobic monomer $NaAMC_{14}S$ could contribute to the network formation and gel intensity because it contains hydrocarbyl groups that participate in hydrophobic associations, including electrostatic interactions and complexation. Finally, all monomers are grafted into SR-14, which has high molecular weight. The intermediate products of SR-14 gel must be hydrolyzed with NaOH to create additional hydrophilic $-COO^-$ or -COOH [19]. By simply mixing the polymerized intermediate products with NaOH under airtight conditions at 90 ℃, sodium hydroxide can participate in a nucleophilic addition elimination reaction with $-CONH_2$ on polymer chains. In this reaction, the transformation of $-CONH_2$ into -COONa is accompanied by the release of ammonia. The water absorbency of the hydrolyzed polymer would then increase as the number of hydrophilic groups, including -OH, -COOH and $-COO^-$.

Fig. 1. The FT-IR spectra of (a) soluble starch, (b) $NaAMC_{14}S$, and (c) soluble starch-*g*-poly(AM-*co*-$NaAMC_{14}S$) (SR-14).

Fig. 2. Schematic of the synthesis of SR-14.

3.1.2. SEM analysis

Figure 3 presents a SEM micrograph of freeze dried SR-14 and its expanded polymer chains after immersion in distilled water. As illustrated in Fig. 3 (a and b), after graft copolymerization, the monomers have formed a multi-layered, dense, microporous network that is supported by large and small chains. The dense network structure allows water molecules to transfer into the interior of resin, and this behavior increases~~d~~ water absorbency and water retention capacity [20]. Figure 3 (c, d) show the micromorphology of freeze dried SR-14 after 5 h of immersion in distilled water. The image shows that the macromolecular chains have expanded. Moreover, the chains have connected to some small branched chains to form a network, so that more and more water molecules are entrapped [21].

Fig. 3. SEM micrographs of (a and b) the SR-14 polymer gel, (c and d) freeze-dried SR-14 after immersion in distrilled water.

3.2. Effects of key conditions on SAR synthesis

3.2.1. Effects of degree of hydrolysis (DH)

The effects of different DH of SAR were investigated. The results are presented in Fig. 4 and demonstrate that hydrolysis is critical for water absorbency. Water absorbency is negligible in the absence of hydrolysis. Specially, it increased linearly when the DH was less than 40 %; slightly increased when the DH ranged from 40 % to 80 %; peaked when the DH was 80%, and decreased when DH exceeded 80 %. By contrast, after hydrolysis, water absorbency in distilled water increased from 31.71 g/g to 1183.43 g/g, when the DH increased from 0 % to 80 %. The results of elemental analysis are shown in Table 1 and confirm that the addition of NaOH result in the transformation of -$CONH_2$ groups to -COO^- and the release of NH_3 [22]. The mass percentages of N changed from 10.28 % before hydrolysis to 1.82 % after hydrolysis, and those of O changed from 33.82 % before hydrolysis to 61.39 % after hydrolysis. The -COO^- content of hydrolyzed polymers is dependent on the amount of NaOH, and it has been reported that the carboxyl content increase with increasing NaOH concentration to reach a maximum and then decrease [23].

Fig. 4. Effects of the degree of hydrolysis on the water absorbency of SR-14.

Table. 1 Elemental analysis of SR-14 before and after hydrolysis (wt, %).

3.2.2. Effects of the soluble starch amount on water absorbency

The effects of soluble starch contents on the water absorbency of SR-14 in distilled water were investigated. The results are shown in Fig. 5(a). Single monomer content accounted for the total monomers percentage (weight 10.0 g). Water absorbency increased from 643.23 g/g to 1614.30 g/g when soluble starch contents increased from 5 % to 40 %. This result is mainly attributed to the increased length of the C-C skeleton and amounts of -OH groups. Synthesized SR-14 with 40 % starch content demonstrates the maximum absorbency. Further increasing the starch ratio reduces water absorbency because of the limitation imposed by AM concentration [24]. Specifically, further increasing soluble starch content reduces the starch to AM ratio and introduces excess starch that could not be grafted by AM. These results confirm that the viscidity of polymeric gel increases sharply at the later stages of polymerization [25].

3.2.3. Effects of AM and NaAMC$_{14}$S amount on water absorbency

A specific hydrophobic monomer NaAMC$_{14}$S is added onto the graft polymerization to enhance the water absorbency of the final SR-14 product. The effects of AM/NaAMC$_{14}$S ratio on the water absorbency of SR-14 are shown in Fig. 5 (b). The soluble starch-*g*-AM polymer had a low water absorbency of 655.66 g/g in the absence of NaAMC$_{14}$S. However, the water absorbency of the SR-14 gel drastically increased to 1198.76 g/g with the addition of NaAMC$_{14}$S. This improvement confirms our hypothesis that introducing NaAMC$_{14}$S into the soluble starch and AM system would drastically increase the water absorbency of the polymerized resin. The introduction of hydrophobic monomers into traditional polymerized systems is an innovative approach for enhancing the performance of SAR.

Soluble starch-*g*-poly(AM-*co*-NaAMC$_{14}$S) samples synthesized under different conditions (SR-14-Q and SR-14-H: SR-14 prepared with the addition of NaAMC$_{14}$S before and after hydrolysis; SR-Q and SR-H: resin prepared with the absence of NaAMC$_{14}$S before and after hydrolysis) were subjected to rheological experiments to illustrate the contribution of NaAMC$_{14}$S to monomer polymerization. Figure 5(e and f) show the response of the polymer gel as a function of frequency in terms of the storage modulus (G′) and loss modulus (G″), respectively. Obviously G′ and G″ increased before and after hydrolysis in the presence of NaAMC$_{14}$S. This result indicates that NaAMC$_{14}$S acts as an additional crosslinking agent that enhances strength of SR-14 [26]. The addition of NaAMC$_{14}$S promotes to the construction of three-dimensional network. Hydrophobic $-(CH_2)_{11}-CH_3$ groups in $NaAMC_{14}S$ promote intramolecular and intermolecular associations in graft polymerization, whereas $-SO_3$ groups induced electrostatic repulsion in the network structure [27]. As a result, the addition of $NaAMC_{14}S$ considerably increases the water absorbency and viscoelasticity of SR-14.

3.3.4. Effects of initiator APS amount on water absorbency

The effects of the initiator APS on water absorbency are shown in Fig. 5 (c). Water absorption capacity gradually increased when the volume of APS was less than 4 mL and drastically decreased when the volume of APS ranged from 4 mL to 7mL. The addition of APS to the pregelatinized starch solution results in the formation of free hydroxymethyl radicals that promote copolymerization among soluble starch, AM, and $NaAMC_{14}S$. APS content is positively associated with free radical quantity, which controls graft polymerization rate. Reducing the initiator concentration reduces the efficiency of graft polymerization. Thus, some molecules are not grafted and ~~were~~ are physically trapped in the gel; these effects result~~ed~~ in the development of a weak network structure [28]. By contrast, increasing the initiator concentration increases free radical quantity~~,~~. This effect then increases polymerization rate, and decreases the molecular mass of the synthesized products.

3.3.5. Effects of MBA content on water absorbency

The effects of the MBA content on water absorbency in graft polymerization were studied by varying the MBA amount from 0.005 g to 0.040 g (Fig. 5 (d)). Fig. 5 (d) shows that increasing the MBA content decreased water absorbency. In terms of the polymerization mechanism, individual monomers would transform into a series of long chains under the action of APS. The addition of MBA result in the formation of numerous intersection points for the development of the three-dimensional network structure. In the presence of insufficient MBA, the swollen gel has low strength and is in a semi-dissolved state, provided the illusion of high water absorbency. In the presence of excess MBA, the swollen gel becomes brittle because extensive cross linking density occur~~red~~ between macromolecular chains; this effect then decreases the specific surface area and water absorbency of the gel [29]. Consequently, the number of cross-links involved in the construction of the three-dimensional network structure is dependent on the content of MBA content that affects the synthesis of SAR.

Fig. 5. Effects of (a) soluble starch content, (b) ratio of AM to $NaAMC_{14}S$, (c) APS volume, (d) MBA amount on the water absorbency of SR-14; Effect of frequency on (e) storage modulus and (f) loss modulus of polymers before and after hydrolysis in the presence and absence of $NaAMC_{14}S$.

3.4. Swelling kinetics of SR-14

The optimal conditions for the graft polymerization of SR-14 were determined through single-factor experiments. The optimal conditions for 50 g polymerization system are as follows: soluble starch content of 40 % (10 g solid content), $AM/NaAMC_{14}S$ ratio of 99.7/0.30, APS volume of 4 mL (5000 mg/L), MBA content of 0.02 g, and DH of 80 %.

Experiments were conducted to study the swelling behavior and maximum water absorbency of SR-14 in distilled water and 0.9 wt.% NaCl solution. The absorption capacity of SR-14 over time was calculated. Figure 6 (a, b) present absorption kinetics of SR-14 in distilled water and in 0.9 wt.% NaCl solution, respectively. The swelling ratio of SR-14 slowly increased during the first 3 hours, and then increased sharply in the following few hours. After 7 h of immersion, the swelling ratio increased gradually, and the maximum water absorbency of 2536.77 g/g was obtained within 11 hours. Equilibrium was then established. The trend exhibited by the swelling ratio in 0.9 wt.% NaCl solution were similar to that exhibited by the swelling ratio of SR-14 in distilled water. The maximum absorbency of 92.98 g/g was obtained within 18 h of immersion in 0.9 wt.% NaCl solution. These results indicate that SR-14 has excellent water absorption and could tolerate high salinity levels. The drastic difference between the maximum water absorbency of SR-14 in distilled water and 0.9 wt.% NaCl solution may be mainly attributed to the presence of Na^+ and Cl^- ions that hinder resin to swell in 0.9 wt.% NaCl solution [30]. The maximum water absorbency of soluble starch-*g*-poly(AM) were 1222.27 g/g and 62.29 g/g in distilled water and 0.9 wt.% NaCl solution, respectively, in the absence of $NaAMC_{14}S$ and under the same other experimental conditions. These results confirm that $NaAMC_{14}S$ can enhance water absorbency and salt resistance in the soluble starch and AM system.

The Fickian diffusion model was utilized to investigate the water absorption behavior of SR-14 in different solutions. The kinetic models are expressed as below:

$$\frac{Q_{at}}{Q_{amax}} = kt^n \qquad (3)$$

Taking the natural logarithm of Equation (3),

$$\ln Q_{at} - \ln Q_{amax} = \ln k + n \ln t \qquad (4)$$

where Q_{amax} (g/g) is the maximum absorption capacity of SR-14, Q_{at} (g/g) is the absorption capacity of SR-14 at time t, t (h) is absorption time, k is the structural parameter of SR-14, and n is the characteristic swelling parameter. $n < 0.5$, $n > 1$, and $0.5 < n < 1$ indicate Fickian diffusion, relaxation diffusion and non-Fickian, respectively [31].

Moreover, k and n were calculated by taking the natural logarithm of Q_a and t. Figure 6 (c) and (d) show the variation in the absorbency of SR-14 in distilled water and 0.9 wt.% NaCl solution, respectively, as a function time.

Swelling behavior in distilled water can be divided into three stages on the basis of line fitting. The first stage involved the relaxation diffusion of macromolecular chains with the initial n of 2.831. The second stage involved Fickian diffusion with the drastically reduced n of 0.258. In the third stage, swelling was in equilibrium state without net water absorbency. These results indicate that macromolecular chains undergo relaxation and stretching during the swelling of SR-14 in distilled water. These behaviors increase the livelihood that hydrophilic groups will adhere to water molecules. Meanwhile, the three dimensional network structure of SR-14 gradually develop, which form an osmotic differential between external surface and internal surface that drive the diffusion of water molecules into the gel. However, the deceleration of the change in Q_a after 7 h of immersion may be primary attributed to the intersection points constraint and anti-ion shielding effect exerted by -COO^- on polymer chains outside the network structure [32]. Numerous water molecules are retained through microscopic dynamic changes, and this process continues for a while.

Similarly, swelling behavior in 0.9 wt.% NaCl solution could be divided into three stages. The diffusion coefficient n changed from 0.884 during the first stage to 0.384 during the second stage and finally stabilized. Swelling behavior during the first 6 h of immersion was characterized as Non-Fickian diffusion and that during the next few hours was characterized as Fickian diffusion. Diffusion reached a low peak after 13 h and then slightly fluctuated. Sodium chloride solute molecules negligibly influence the swelling of SR-14 in 0.9 wt.% NaCl solution because the resin particles have fine internal structures. The swelling of SR-14 in 0.9 wt.% NaCl solution mainly occurs through water diffusion. After macromolecular chain relaxation, polymer groups, such as -COOH and -COONa, are ionized into -COO$^-$ and Na$^+$. The presence of numerous Na$^+$ ions in the solution would inhibit ionization and considerably reduce resin expansion [33]. As a result the water absorbency of SR-14 in the distilled water was 27-fold higher than that in 0.9 wt.% NaCl solution.

Fig. 6. Swelling kinetics of SR-14 (a, c) in distilled water and (b, d) 0.9 wt.% NaCl solution.

3.5. Expansion of SR-14

The ALLIED camera was used to photograph the outlines of expanded SR-14. As illustrated in Fig. 7, once immersed in distilled water, SR-14 began to swell in all directions because of the difference between water osmotic pressure and Na$^+$ concentration. As inferred from the experimental results for the swelling kinetics of

SR-14 in distilled water, -COONa groups would be gradually ionized to release Na^+ into the solution. The Na^+ diffusion rate would later decelerate in the later stage of expansion. This behavior reduces the driving force available for water molecule migration. After 45 min, the rate of outward expansion decelerated. Meanwhile, the gel split into pieces and gradually collapsed in an expanding circular pattern. Finally, excess water was retained in the gel.

Fig. 7. ALLIED camera images (40×) showing the expansion of SR-14 in distilled water.

4.Conclusion

By adding a hydrophobic monomer $NaAMC_{14}S$, the super absorbent resin Soluble starch-*g*-poly(AM-*co*-$NaAMC_{14}S$) (SR-14) was successfully synthesized in aqueous solution through graft polymerization. The introduction of NaOH-induced hydrolysis to the last stage of gel polymerization can enhance the water absorbency of the AM system, and the DH values of 0 % to 80 % drastically increased the water absorbency of SR-14 from 31.71 g/g to 1183.43 g/g in distilled water. This result indicates that subjecting AM polymerization systems to hydrolysis improved the water absorbency of the final SAR. The maximum water absorbency of SR-14 were 2536.77 g/g and 92.98 g/g in distilled water and 0.9 wt.% NaCl solution, respectively. The swelling process of SR-14 showed good fittings of water absorbency data to Fickian diffusion model. FT-IR, rheological, and water absorbency analyses revealed that the addition of $NaAMC_{14}S$ considerably improved the mechanical properties and absorption capacity of SR-14. These improvements can be mainly attributed to the hydrophobic association of $NaAMC_{14}S$. In the absence of $NaAMC_{14}S$, the water absorbency of soluble starch-*g*-poly(AM) decreased to 1222.27 g/g in distilled water and 62.29 g/g in 0.9 wt.% NaCl solution. This study demonstrates that the addition of $NaAMC_{14}S$ is an innovative approach for enhancing the water absorbency of SAR.

Acknowledgements

The authors would like to thank the financial support provided by the Demonstration Project of Sichuan Provincial Science and Technology Department (18ZDYF0051). The authors would like to thank the very useful suggestions from the editors and reviewers.

Rferences

[1] H. J. Kim, J. M. Koo, S. H. Kim, S. Y. Hwang, Polym. Degradation and Stability **2017**, *144*, 128.

[2] S. Sharma, A. Dua, A. Malik, Europ. Polym. J. **2014**, *59*, 363.

[3] N. Chaukura, W. Gwenzi, T. Bunhu, D. Ruziwa, I. Pumure, Resour. Conser. & Recy. **2016**, *107*, 157.

[4] S. F. Zhang, W. Wang, H. Y. Wang, W. Y. Qi, L. Yue, Q. F. Ye, Carbohydrate Polym. **2013**, *101*, 798.

[5] Q. Huo, D. Liu, J. J. Zhao, J. S. Li, R. N. Chen, S. Y. Liu, Starch-Stärke **2017**, *69*, 11.

[6] J. Li, J. Ji, J. Xia, B. Li, Carbohydrate Polym. **2012**, *87*, 757.

[7] B. J. Gao, L. D. Jiang, D. L. Kong, Colloid and Polym. Sci. **2007**, *285*, 839.

[8] J. Shu, X. J. Li, D. B. Zhao, Adv. Mater. Res. **2009**, *148*, 799.

[9] J. Y. Chen, M. Jiang, Y. X. Zhang, H. Zhou, Macromolecules **1999**, *32*, 4861.

[10] J. Ma, P. Cui, L. Zhao, R. H. Huang, Europ. Polym. J. **2002**, *38*, 1627.

[11] C. Wang, X. R. Li, P. Z. Li, Y. H. Niu, X. W. Yang, J. of Polym. Res. **2013**, *20*, 147.

[12] V. D. Athawale, V. Lele, Starch - Stärke **2015**, *53*, 7.

[13] H. C. Ge, S. K. Wang, Carbohydrate Polym. **2014**, *113*, 296.

[14] M. D. Teli, N.G. Waghmare, Carbohydrate Polym. **2010**, *81*, 695.

[15] Y. Z. Jiang, B. C. Liu, J. K. Xu, K. L. Pan, H. J. Hou, J. P. Hu, J. K. Yang, Carbohydrate Polym. **2018**, *182*, 106.

[16] A. Sawut, M. Yimit, W. Sun, I. Nurulla, Carbohydrate Polym. **2014**, *101*, 231.

[17] Y. X. Chen, S. Y. Liu, G. Y. Wang, Polym. Composites **2007**, *28*, 47.

[18] N. Mohammad, Y. Atassi, M. Tally, Polym. Bulletin **2017**, *74*, 4453.

[19] Y. Zhao, T. W. Tan, Macromoleculer Chem. and Phys. **2006**, *207*, 1297.

[20] Y. Bao, J. Z. Ma, N. Li, Carbohydrate Polym. **2011**, *84*, 76.

[21] S. Riyazi, J. T. Kevern, M. Mulheron, Constr. and Building Mater. **2017**, *147*, 669.

[22] M. Sadeghi, H. Hosseinzadeh, J. of Appied Polym. Sci. **2008**, *108*, 1142.

[23] M. I. Khalil, S. Farag, K. M. Mostafa, A. Hebeish, Starch - Stärke **1994**, *46*, 312.

[24] J. X. Zhang, F. S. Wang, B. Wang, H. X. Li, Applied Mech. and Mater. **2013**, *295-298*, 3067.

[25] K. M. Mostafa, Polym. Degradation & Stability **1997**, *55*, 125.

[26] J. Maity, S. K. Ray, Carbohydrate Polym. **2018**, *182*, 159.

[27] C. Tsitsilianis, I. Iliopoulos, G. Ducouret, Macromolecules **2000**, *33*, 2936.

[28] R. J. Wang, L. W. Yang, H. D. Zhang, T. J. Geng, Adv. Mater. Res. **2013**, *873*, 708.

[29] Z. Ma, Q. Li, Q. Yue, B. Gao, X. Xu, Q. Zhong, Bioresource Technol. **2011**, *10*, 2853.

[30] Y. Zhao, H. Su, L. Fang, T. Tan, Polym. **2005**, *46*, 5368.

[31] A. E. Aissaoui, A. E. Afif, J. of Membrane Sci. **2017**, *543*, 172.

[32] R. K. Arya, K. Tewari, S. Shukla, Progress in Organic Coatings **2016**, *95*, 8.

[33] W. Kong, Q. Li, J. Liu, X. Li, L. Zhao, Y. Su, Q. Yue, B. Gao, RSC Adv. **2016**, *6*, 83234.

Figure legends

Fig. 1. The FT-IR spectra of (a) soluble starch, (b) $NaAMC_{14}S$, and (c) soluble starch-*g*-poly(AM-*co*-$NaAMC_{14}S$) (SR-14).

Fig. 2. Schematic of the synthesis of SR-14.

Fig. 3. SEM micrographs of (a and b) the SR-14 polymer gel, (c and d) freeze-dried SR-14 after immersion in distrilled water.

Fig. 4. Effects of the degree of hydrolysis on the water absorbency of SR-14.

Fig. 5. Effects of (a) soluble starch content, (b) ratio of AM to $NaAMC_{14}S$, (c) APS volume, (d) MBA amount on the water absorbency of SR-14; Effect of frequency on (e) storage modulus and (f) loss modulus of polymers before and after hydrolysis in the presence and absence of $NaAMC_{14}S$.

Fig. 6. Swelling kinetics of SR-14 (a, c) in distilled water and (b, d) 0.9 wt.% NaCl solution.

Fig. 7. ALLIED camera images (40×） showing the expansion of SR-14 in distilled water.

Table legends

Table. 1 The result of elemental analysis of SR-14 before and after hydrolysis (wt, %).

Table. 1 The result of elemental analysis of SR-14 before and after hydrolysis (wt, %)

	N/%	C/%	S/%	H/%	O/%
Before hydrolysis	10.28	43.64	0.13	12.15	33.82
After hydrolysis	1.82	29.55	0.08	7.16	61.39

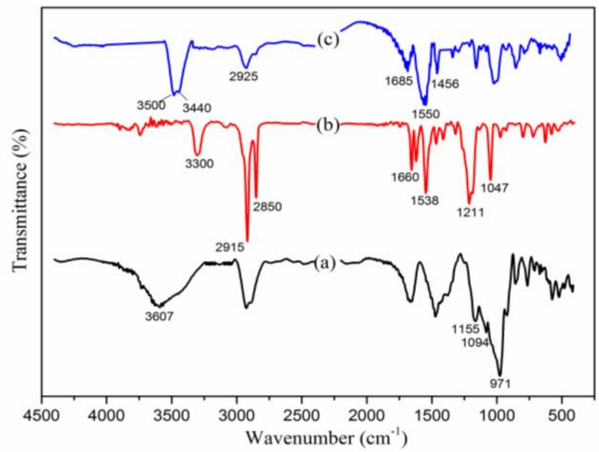

Fig. 1. The FT-IR spectra of (a) soluble starch, (b) NaAMC$_{14}$S, and (c) soluble starch-*g*-poly(AM-*co*-NaAMC$_{14}$S) (SR-14).

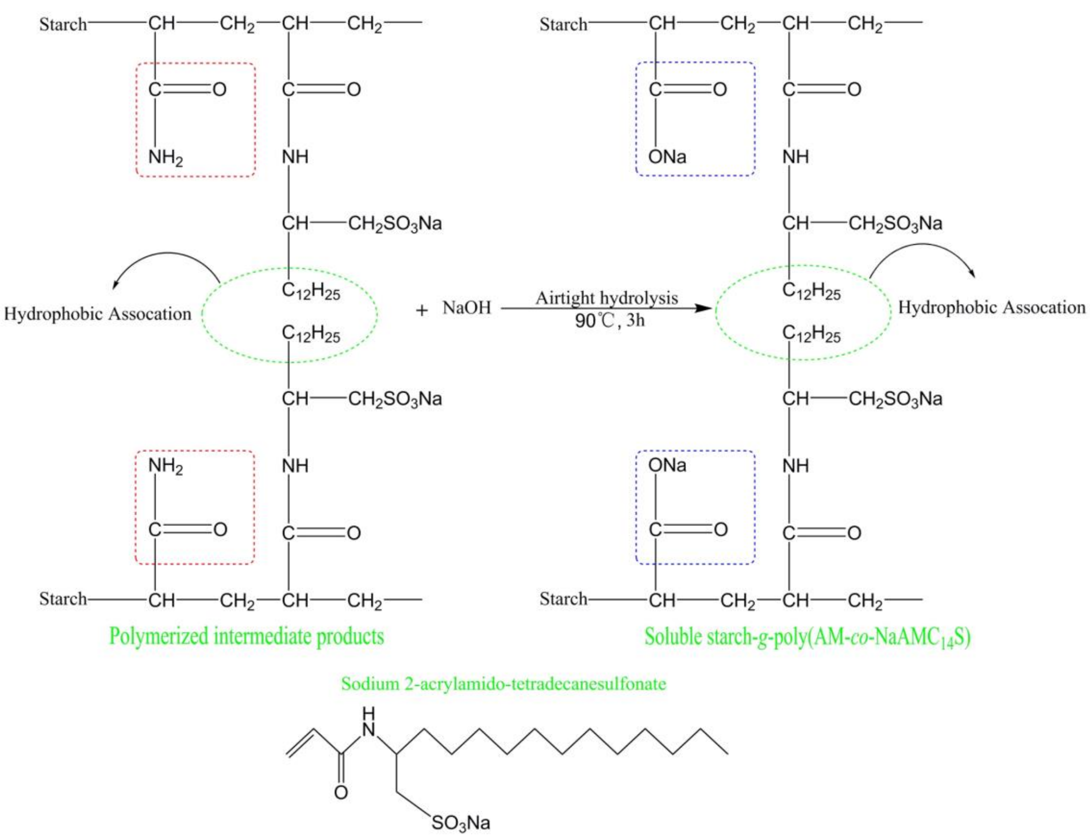

Fig. 2. Schematic of the synthesis of SR-14.

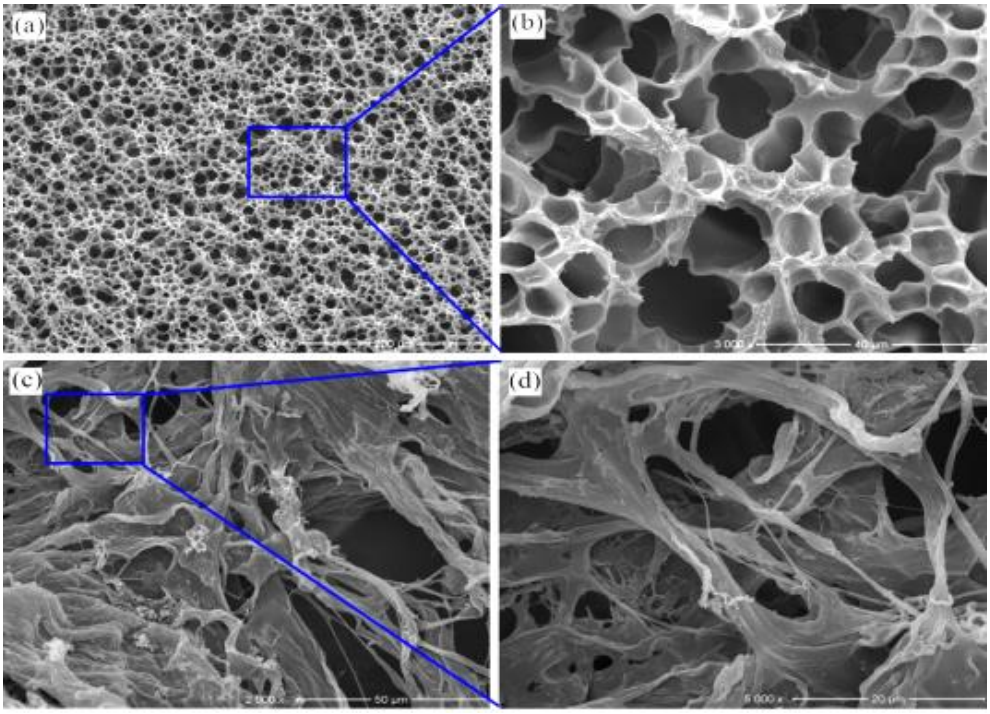

Fig. 3. SEM micrographs of (a and b) the SR-14 polymer gel, (c and d) freeze-dried SR-14 after immersion in distrilled water.

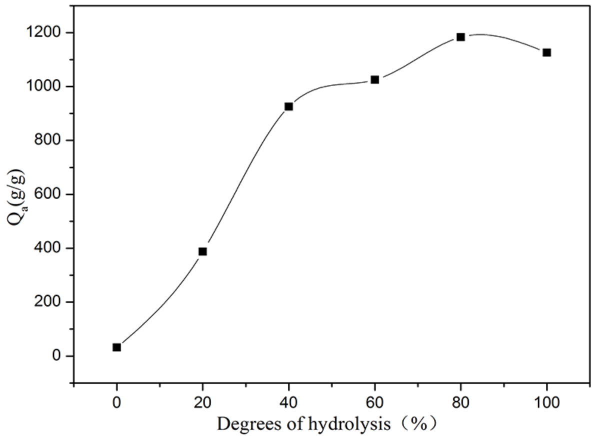

Fig. 4. Effects of the degree of hydrolysis on the water absorbency of SR-14.

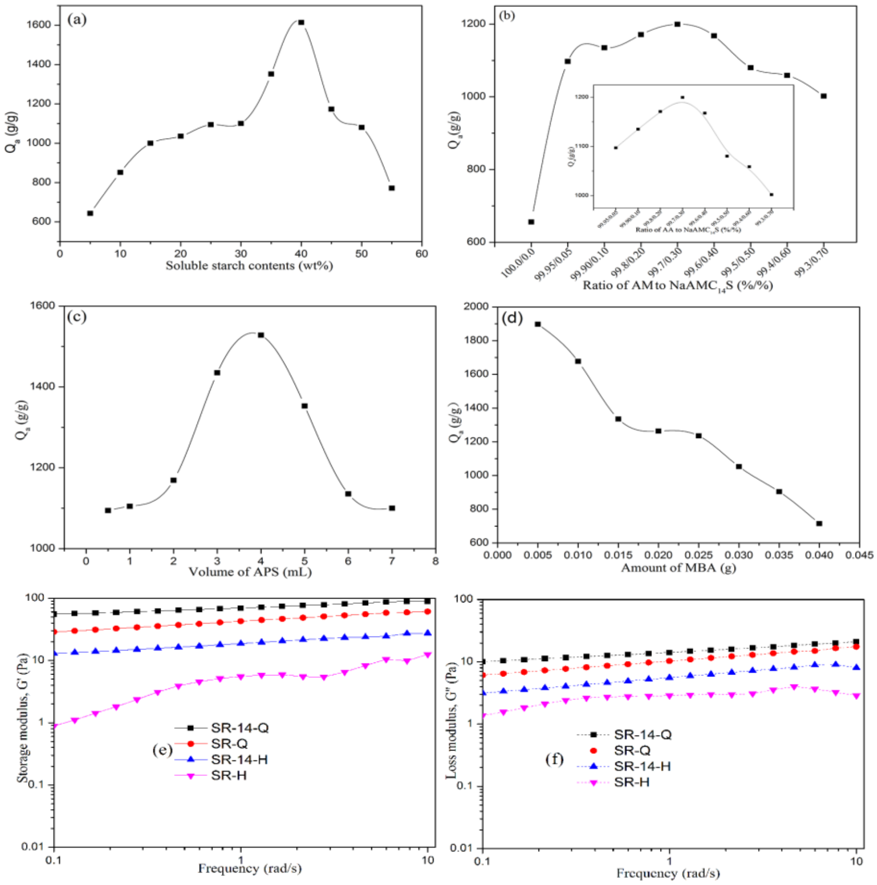

Fig. 5. Effects of (a) soluble starch content, (b) ratio of AM to NaAMC$_{14}$S, (c) APS volume, (d) MBA amount on the water absorbency of SR-14; Effect of frequency on (e) storage modulus and (f) loss modulus of polymers before and after hydrolysis in the presence and absence of NaAMC$_{14}$S.

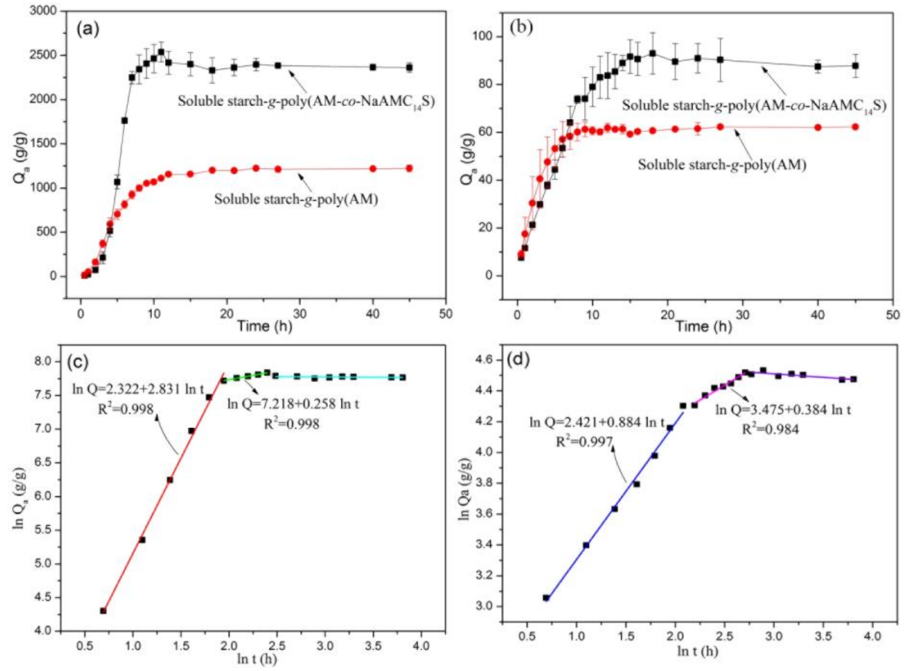

Fig. 6. Swelling kinetics of SR-14 (a, c) in distilled water and (b, d) 0.9 wt.% NaCl solution.

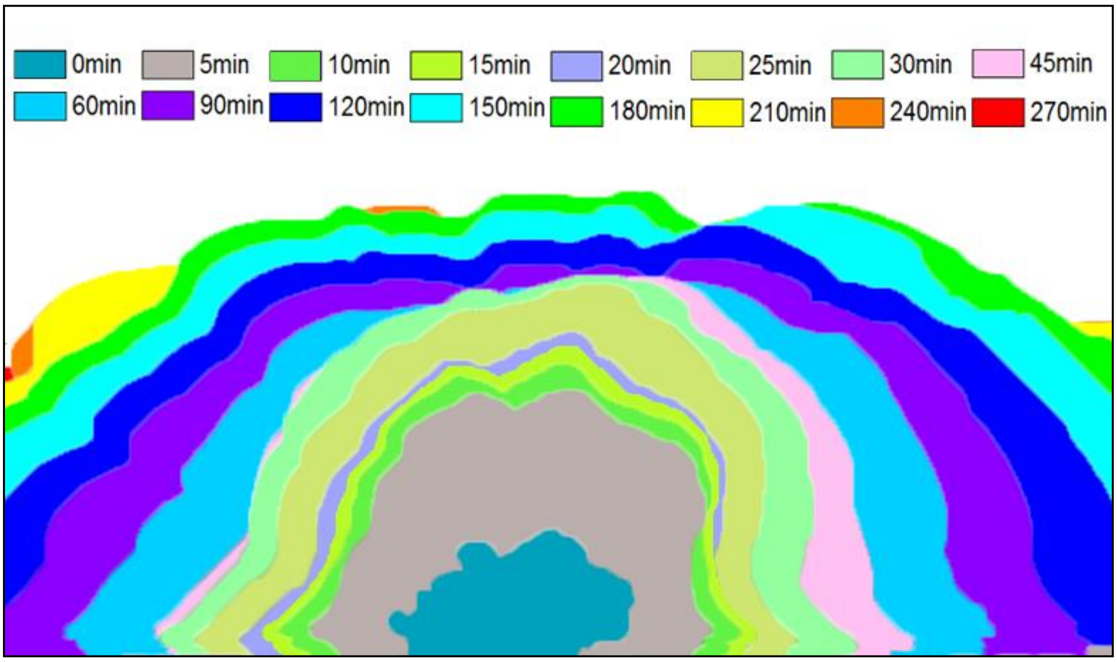

Fig. 7. ALLIED camera images (40×) showing the expansion of SR-14 in distilled water.